

Suppression of Entangled Diblock Copolymer Diffusion at and below the Order–Disorder Transition

Marina Guenza,[†] Hai Tang, and
Kenneth S. Schweizer*

Departments of Materials Science & Engineering and
Chemistry, and Materials Research Laboratory, University
of Illinois, 1304 West Green Street, Urbana, Illinois 61801

Received February 3, 1997

Revised Manuscript Received April 7, 1997

The structure, order–disorder transition (ODT), and dynamics of self-assembling diblock copolymer melts has been intensely studied in recent years.^{1,2} Microdomain scale fluctuations strongly influence equilibrium properties above and below the ODT and are rather well accounted for by coarse-grained field theory (BLFH)³ and liquid state polymer reference interaction site model (PRISM) theory.^{4,5} For unentangled, short diblocks, the influence of microdomain formation on translational diffusion appears to be weak.^{6,7} However, transport of entangled diblocks is significantly retarded, becoming slower as the degree of polymerization and/or segregation increases, thereby indicating a strong coupling of entanglement constraints and thermodynamically-driven microphase separation.^{6,8,9}

We have recently developed a microscopic polymer-mode coupling (PMC) theory of diffusion in entangled blends¹⁰ and diblock copolymer¹¹ liquids which is a natural extension of the successful PMC theory of homopolymer solutions and melts.^{12,13} This theory provides a good description¹¹ of self-diffusion and tracer diffusion measurements for quenched samples^{6,8} of entangled symmetric copolymer polyolefin melts above, and slightly below, the ODT. More recently, Lodge and co-workers⁹ have performed measurements over a much wider range of degree of polymerization and segregation conditions for shear-aligned lamellar microstructure samples. Rather surprisingly, the measured self-diffusion tensor exhibited modest anisotropy. Two distinctive regimes of diffusion suppression were observed: a thermally activated behavior, followed by a temperature-independent regime under the strongest segregation conditions where a factor of ≈ 100 reduction of the diffusion constant due to microdomain formation was observed. Qualitative interpretations were advanced on the basis of “activated reptation”^{9,14} and “entropic arm-retraction” motional mechanisms.⁹

The primary goal of this communication is generalize and apply the PMC theory to simultaneously treat diblock copolymer self-diffusion above and well below the ODT. This requires combining the PRISM theory of diblock melts,⁵ including recent extensions to estimate the location of the ODT and quantitatively describe scattering data,¹⁵ with the PMC approach. New dynamic scaling laws are derived, and both model calculations and quantitative applications to experiments are presented. Our work represents the first general treatment of the entangled copolymer problem and comparison with recent experiments. Predictions for the chain relaxation time relevant to viscoelastic and dielectric

measurements, and diblock tracer diffusion, are also briefly discussed.

The simplest “structurally, interaction, compositionally, and dynamically symmetric” model is adopted.^{5,11} The AB diblocks are uncrossable Gaussian chains of N segments, of equimolar $f = 1/2$ composition, identical segment lengths $\sigma = d$ (hard core diameter), a repulsive tail potential $v_{AB}(r)$ is adopted corresponding to a positive bare enthalpic χ -parameter, and a single segmental friction constant ζ_0 , which characterizes the unentangled Rouse dynamics. The compressible melt has a reduced segment density $\rho\sigma^3$, or equivalently a density screening (or “packing”) length⁵ $\xi_p = 3/(\pi\rho\sigma^2)$.

Both PRISM and PMC theories are based on an isotropic liquid description. The self-diffusion constant is $D = (\beta\zeta N)^{-1}$, where $\beta = (k_B T)^{-1}$ and ζ is the total friction constant per segment. Although not literally true below the ODT, the isotropic model is consistent with the PMC treatment of entanglements. Moreover, it seems reasonable on the basis of the experimental observations of (i) no discontinuity of D at the ODT,^{6–9,16} (ii) strong (isotropic) fluctuations near and below the ODT,¹ (iii) weak anisotropy of D in shear-aligned samples,^{8,9} and (iv) similarity of D measured in some quenched and oriented samples.^{8,9} PMC theory computes the additional friction due to time-correlated intermolecular forces felt by a tagged copolymer. Based on a projection scheme (denoted below by a superscript “Q”) that (approximately) extracts the influence of slow dynamical processes and structural constraints, the general result is^{10,11}

$$\begin{aligned}\zeta &= \zeta_0 + \frac{1}{N_{\alpha,\gamma}} \int_0^\infty dt \langle \mathbf{F}_\alpha(0) \cdot \mathbf{F}_\gamma^Q(t) \rangle \\ &= \zeta_0 + \left(\frac{\rho}{6\pi^2\beta} \right) \int_0^\infty dt \int_0^\infty dk k^4 \sum_{M,M'} \omega_{MM'}^Q(k,t) \times \\ &\quad \left\{ \sum_{p,p'} C_{Mp}(k) S_{pp'}^Q(k,t) C_{pM'}(k) \right\} \\ &= \zeta_0 + \left(\frac{-C_0}{6\pi^2\beta} \right) \int_0^\infty dt \int_0^\infty dk k^4 \sum_{M,M'} \omega_{MM'}^Q(k,t) \quad (1)\end{aligned}$$

The first equality is an exact formal expression where $\mathbf{F}_\alpha(t)$ is the total force exerted on segment α of the tagged chain by all segments on matrix copolymers. The second line follows from the basic PMC theory approximations.^{12,13} The wavevector integrals quantify contributions to the friction associated with correlated dynamical processes on a length scale $2\pi/k$, and the sums are over species type (A or B). For $t = 0$ the term in braces is the medium-induced “potential-of-mean force”, $W_{MM'}$, between tagged diblock segments of type M and M' induced by interactions with the surrounding melt.¹⁷ The latter are described by renormalized effective potentials (or direct correlation functions) $C_{MM'} = C_0 + (1 - \delta_{MM'})\rho^{-1}\chi$, where C_0 is the $k = 0$ value of the repulsive (hard core) contribution and χ is the effective χ -parameter.⁵ $W_{MM'}$ has both total density and concentration fluctuation components.^{10,11,17}

The fluctuating force time correlations decay via collective melt motions, as described by the (projected) dynamic structure factor $S_{MM'}^Q(k,t)$, and via single tagged copolymer motions, as described by the intramolecular dynamic structure factors $\omega_{MM'}^Q(k,t)$. In the

[†] Permanent address: Istituto di Studi Chimico-Fisici di Macromolecole Sintetiche e Naturali, IMAG, National Research Council, Via de Marini 6, Genova, Italy.

homopolymer limit, $\chi \rightarrow 0$, and the entangled athermal melt theory is recovered, where the fluctuating forces are mediated solely by matrix density fluctuations described by⁴ $S_0(k) \equiv S_0(k=0) \equiv S_0 = 12(\xi_\rho/\sigma)^2$. The latter simplifications apply since a one-component melt is homogeneous on the dynamically relevant polymer radius-of-gyration length scale $R_g = \sigma(N/6)^{1/2} \gg \xi_\rho$. The final approximate equality in eq 1 follows for the copolymer problem from the fact⁵ that $N^{-1} \propto \chi \ll -C_0$, $S_0 = (-\rho C_0)^{-1}$ for large N , and a dynamically "frozen matrix" (no "constraint release") assumption, $S_{MM}^Q(k, t) \equiv S_{MM}(k)$; it is formally identical to the entangled homopolymer melt result *except* the decay of the entanglement forces via probe copolymer motion is *influenced by physical clustering and microdomain formation*. The dominant length scale for N -dependent friction coefficient renormalization is R_g , which is proportional to the microdomain scale $2\pi/k^*$. Thus, thermodynamic segregation constraints couple strongly to the relaxation of the hard core entanglement forces. Note that if the excluded volume forces are ignored in eq 1, and only the (small) contribution due to χ is retained, plus the dynamic propagators appropriate for Rouse chains are employed, then we recover the perturbative theory of *unentangled* copolymer diffusion of Leibig and Fredrickson.¹⁸ If the Rouse propagator is employed in eq 1, then one recovers a PMC treatment appropriate^{10,11} for unentangled diblocks, as discussed by Genz and Vilgis.¹⁹

Explicit evaluation of eq 1 requires the projected dynamics of the tagged copolymer in the melt. Following precisely the same approximate scheme successfully developed for the entangled homopolymer problem, we employ the so-called "renormalized Rouse" (RR) model¹² formulated in terms of the bare excluded volume forces as generalized to the symmetric diblock copolymer case.¹¹ The simple dynamic RPA form²⁰ for the RR propagator is employed, $\omega_{MM}^Q(k, t) \equiv \omega_{MM}^Q(k) \exp[-k^2 t / \beta \zeta_{RR} \omega(k)]$, where $\omega(k)$ is the total single chain (Gaussian) structure factor and the effective RR friction coefficient ζ_{RR} is given by

$$\begin{aligned} \zeta_{RR} &= \zeta_0 + \frac{8\sigma^4}{3\beta} \rho \int_0^\infty dt \int_0^\infty dk k^2 j_1^2(k\sigma) \sum_{M,M'} [\omega_{M,M'}^Q(k, t) \times \\ &\quad \sum_{p,p'} g_{Mp}(\sigma) S_{pp'}^Q(k, t) g_{p'M'}(\sigma)] \\ &= \zeta_0 + \frac{2\sigma^4}{3\beta} \rho \int_0^\infty dt \int_0^\infty dk k^2 j_1^2(k\sigma) \left[\sum_{M,M'} \omega_{M,M'}^Q(k, t) \right. \\ &\quad \left. \{4g_0^2(\sigma) S_0 + (\Delta g(\sigma))^2 S_\phi(k)\} \right] \\ &\propto \zeta_0 \rho g_0^2(\sigma) S_0 \sqrt{N} [1 + \lambda J] \end{aligned} \quad (2)$$

Here, $j_1(x)$ is the first spherical Bessel function, $g_{MM'}(\sigma)$ is the intermolecular pair correlation function between segments of species M and M' on different chains *at the contact distance relevant to the hard core repulsion*, and the projected propagator is given by Rouse dynamics. The two terms in curly braces describe the contributions of density and concentration fluctuation mediated excluded volume forces, respectively. The former are spatially local in a dense fluid and hence constrain the four mutually interacting segments on the tagged copolymer and surrounding matrix to be spatially close, consistent with qualitative notions about entanglements. In contrast, concentration fluctuations are spatially correlated over large distances and hence can

induce dynamical correlations of tagged copolymer segments that are widely separated in space. Microdomain formation enters the force time correlations via *local* physical clustering, as quantified by the contact value of $\Delta g = g_{AA} + g_{BB} - 2g_{AB}$, and the concentration fluctuation collective structure $S_\phi(k)$. In PRISM theory for symmetric chain models,^{4,5} the RPA form²¹ applies: $S_\phi(k) = (F(k) - 2\chi)^{-1}$, where χ is fluctuation renormalized and $F(k)$ is a known combination of copolymer partial structure factors where $F(k^*) \propto N^{-1}$.

The final proportionality in eq 2 applies for well-entangled chains and implicitly defines the factor $J = \mathcal{J}(T, N, f, \rho, \xi_\rho)$ as the ratio of the concentration fluctuation mediated to density fluctuation mediated friction constants. A numerical factor " λ " has been introduced to account for our expected inability to accurately compute the *absolute magnitude* of friction within PMC theory and the oversimplified symmetric diblock model employed. Although one might hope that λ is independent of material parameters, in practice the simplified nature of the theory may require it to depend on nonuniversal properties such as f , ξ_ρ , and N_e (but *not* N or T) in quantitative applications to experimental data. The quantity $\rho g_0^2 S_0$ is proportional to the mean square excluded volume force exerted by the matrix polymers on a tagged segment, while the $N^{1/2}$ factor is of geometric origin and proportional to the number of "contacts" between a pair of interpenetrating coils in three-dimensions.¹³

Using eq 2 in eq 1 yields for *entangled* copolymers

$$D = \frac{N_D}{\beta \xi_0 N^2 (1 + \lambda J)} \equiv \frac{D_0}{1 + \lambda J} \quad (3)$$

where $N_D \propto [g_0(\sigma)]^{-2}$ is a system-specific crossover degree of polymerization from unentangled to entangled diffusion¹³ and D_0 is a reference diffusion constant unaffected by concentration fluctuations corresponding to the $\chi \rightarrow 0$ limit. Based on the dominant one-wavevector description of microdomain scale concentration fluctuation,^{3,5} eq 2 predicts $J \propto (\Delta g(\sigma)/\xi_\rho)^2 \sqrt{S^* N}$, where S^* is the peak intensity $S_\phi(k^*)$. The factor $(1 + \lambda J)$ also represents the enhancement of the longest conformational relaxation time of the chain due to the slowing down of entanglement force time correlations associated with microdomain formation. For the symmetric model, this connection is precise since PMC theory predicts²² a "Fick's law" type relation, $\tau \propto R_g^2/D$, where τ is the terminal chain relaxation time that controls the frequency of the stress or dielectric loss modulus maximum.

Analytic scaling laws follow from eqs 2 and 3 plus the known dependence of S^* and Δg on temperature and N as predicted by diblock Gaussian thread copolymer PRISM theory.^{5,11,15} A representative example for S^* , including comparison to experimental scattering data, is shown in Figure 1. The general calculation, and behavior in limiting cases, of S^* and an apparent ODT temperature, T_{ODT} , have been discussed elsewhere.^{5,15} One finds $S^* \propto N(T \gg T_{ODT})$, $N^{1/3}(T = T_{ODT})$, and $N^2(T \ll T_{ODT})$. The local clustering function is given by¹⁰ $\Delta g = g_{AA} + g_{BB} - 2g_{AB} \cong (12/\pi\rho\sigma^3)(1/\sqrt{N})[12\sqrt{S^*/N} - \sqrt{3N/S^*} + \sqrt{6\chi_s N} - 12/\sqrt{2\chi_s N}]$, which vanishes as $\chi \rightarrow 0$, and where $\chi = \chi_s - (2S^*)^{-1}$ with χ_s equal to the critical value (10.495 for $f = 1/2$). Combining these results yields $\Delta g \propto N^{-1/2}(T \gg T_{ODT})$, $N^{-1/3}(T = T_{ODT})$, and $N^0(T \ll T_{ODT})$. The low-temperature result is physically sensible for a highly segregated *liquid* composed of nearly pure A and B microdomains. The frictional enhancement

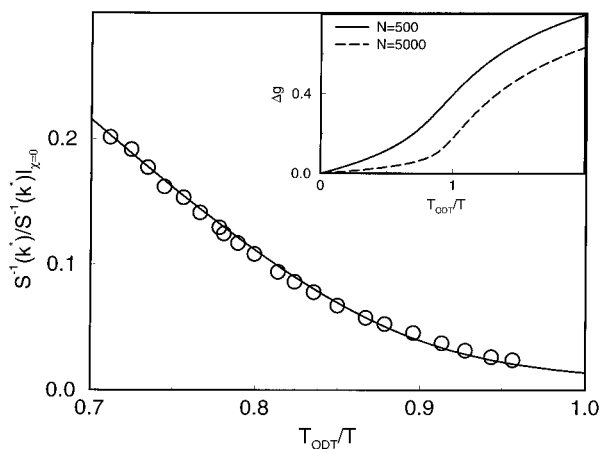


Figure 1. Best fit (with $\xi_p/\sigma = 0.14$) of PRISM theory (full line) to experimental inverse peak static structure factor data for a symmetric PEP-PEE melt of $N = 791$ (see ref 14). The inset shows model calculations for the local clustering function based on $f = 0.5$, $\xi_p/\sigma = 0.3$.

factor J grows as the amplitude of both long wavelength concentration fluctuations and local physical clustering increase and obeys the qualitative power laws: $J \propto (S^*/N)^{3/2} \propto N^0 (T \gg T_{\text{ODT}})$, $N^{1/2} (T = T_{\text{ODT}})$, and $N^{3/2} (T \ll T_{\text{ODT}})$. The entangled homopolymer law of $D \propto N^{-2}$ is predicted far from the ODT. However, for large N , new scaling exponents emerge at and below the ODT: $D \propto N^{-5/2} (T = T_{\text{ODT}})$ and $N^{-7/2} (T \ll T_{\text{ODT}})$. The latter novel prediction follows from the “ground state” PRISM description of the low-temperature segregated structure.⁵ In strong contrast, *isotropic* BLFH theory³ predicts $S^* \propto N^2/(NT)^2$ at $T \ll T_{\text{ODT}}$. This yields $D \propto N^{-11/2} T^3$, corresponding to a *much smaller* diffusion constant that decreases much faster with N , is strongly temperature-dependent, and *vanishes* as $T \rightarrow 0$.

Following the experimentalists,^{6–9} the ratio D/D_0 is employed to quantify diffusion suppression, where D_0 is defined in eq 3. For viscoelastic or dielectric experiments, the relevant ratio is $\tau/\tau_0 \approx (D_0/D)(R_g/R_{g0})$.² The fundamental prediction of our theory is the existence of three distinct dynamical regimes. (1) Far from the ODT the concentration fluctuations have essentially no effect; i.e. $D/D_0 \approx 1$ and is T -independent. (2) As the ODT is approached, and somewhat below it, D/D_0 decreases rapidly due to enhanced physical clustering and microdomain formation, and a strong thermal dependence on the diffusion suppression emerges. The precise magnitude and T dependence of D/D_0 is *not* expected to be universal since it is influenced by system-specific equilibrium structure and entanglement characteristics of the chains. (3) Well below the ODT, where the local clustering and microdomain scale concentration fluctuations tend to saturate at their strongly segregated values, D/D_0 approaches a minimum (non-universal) value proportional to $N^{-3/2}$, which is T -independent. This is suggestive of an “entropic” transport mechanism, although PMC theory focuses on the ensemble-averaged friction and not the copolymer trajectories. This three-regime scenario is in excellent qualitative agreement with recent experiments.⁹ The fundamental physical content is that the thermodynamic desire to keep the A and B segments segregated prolongs the relaxation time of the fluctuating entanglement forces, which slows down copolymer translational diffusion and conformational relaxation.

Model calculations of J and D/D_0 , which exhibit the three limiting regimes, and crossovers between them, are shown in Figure 2. A meltlike density screening

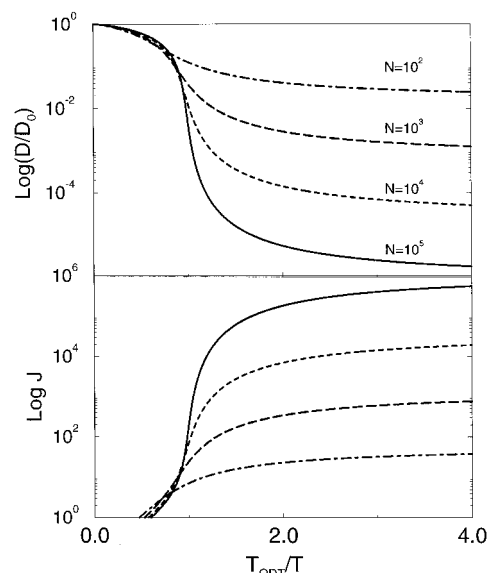


Figure 2. Log-linear plot of the normalized diffusion coefficient and the factor J as a function of normalized inverse temperature for $f = 1/2$, several values of N , $\xi_p/\sigma = 0.3$, and $\lambda = 0.07$.

length¹⁵ of $\xi_p/\sigma = 0.3$ and $\lambda = 0.07$ (see below) were employed. At intermediate temperatures the reduced diffusion coefficient decreases in an approximately *exponential* manner, consistent with the “thermally-activated” interpretation of the data.⁹ The corresponding “apparent activation energy” is predicted to be a (relatively weakly) increasing function of N , which reflects the fact that T/T_{ODT} is not a perfect scaling variable for the concentration fluctuation mediated frictional enhancement.

We have applied the theory to recent self-diffusion measurements on four well-entangled, $f \approx 1/2$ PEP-PEE polyolefin melts.^{6,8,9} The first comparison is for two quenched (globally isotropic) materials:^{6,8} PEP-PEE1 ($N = 562$ based on $M_{\text{segment}} = 56$ g/mol) and PEP-PEE2 ($N = 895$). In the experimental temperature range, PEP-PEE1 is well above its $T_{\text{ODT}} \approx -41$ °C and presumed to obey entangled homopolymer dynamics *unaffected* by long range concentration fluctuations. PEP-PEE2 has a $T_{\text{ODT}} \approx 96$ °C, and the corresponding D_0 was estimated by scaling the measured PEP-PEE1 diffusion constant by the factor $(562/895)^2$, appropriate for entangled homopolymer melts. These data are shown in the top panel of Figure 3, along with D for PEP-PEE2, which falls increasingly *below* the entangled homopolymer value as the material is cooled. Theoretically, we follow the same analysis procedure sketched above and elsewhere;¹¹ $D_0(T, N)$ is determined from the experimental PEP-PEE1 data.^{6,8} A best fit of eq 3 to the PEP-PEE2 data is obtained by varying the numerical factor λ and density screening length. The best fit values are $\lambda = 0.07$ and $\xi_p/\sigma = 0.3$, and the predicted temperature dependence is in excellent agreement with the data. Since experimental-based estimates of the nonuniversal *melt* scaling (or packing) length are ≈ 1 – 5 Å,²³ the fit value of $\xi_p = 0.3\sigma$ falls in the expected range based on typical statistical segment length values.

A much more severe test of the theory is the most recent data for oriented PEP-PEE materials.⁹ This study included PEP-PEE2 plus two higher molecular weight samples, PEP-PEE3 ($N = 1450$, $T_{\text{ODT}} \approx 291$ °C) and PEP-PEE4 ($N = 1970$, $T_{\text{ODT}} \approx 500$ °C). The “parallel” self-diffusion constant data versus reduced

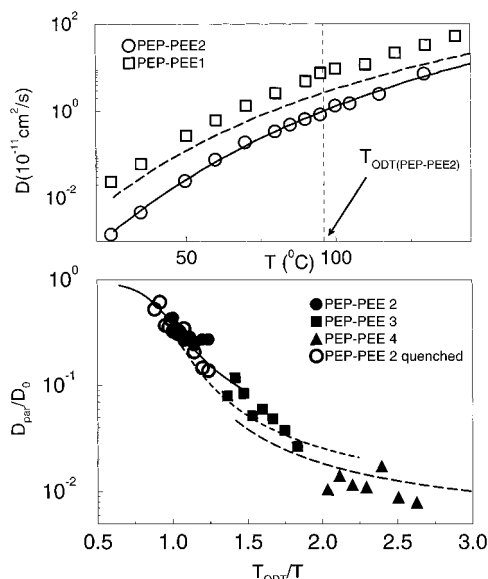


Figure 3. (Top panel) Comparison of the best fit theory (full lines) to experimental data^{6,8} for quenched samples of PEP-PEE2. Data for PEP-PEE1 and the estimated entangled homopolymer curve for PEP-PEE2 (dashed curve) are also shown. These quenched sample data were previously analyzed¹¹ using PMC theory but with BLFH theory as the equilibrium input. (Bottom panel) Comparison of theory (same λ and ξ_p/σ values as in the top plot) with normalized parallel diffusion constant data of shear-aligned samples.⁹ The data for a quenched PEP-PEE2 sample^{6,8} are also shown.

temperature are shown in the bottom panel of Figure 3. The measured anisotropy of the diffusion constants was small (factor of ≈ 2 –3 or much less) and is ignored in our isotropic theory. Note the quenched and aligned PEP-PEE2 data are indistinguishable to within experimental error. Our corresponding PMC predictions are based on *exactly the same* values of λ and ξ_p/σ extracted from analysis of the *quenched* PEP-PEE2 data. We emphasize these results are *not a fit*. The agreement of theory and experiment is very good, especially considering the simplicity of the theory and the large factor of 100 reduction of diffusion observed under relatively strong segregation conditions.

Prior theoretical work (employing BLFH equilibrium input)¹¹ for PEP-PEE diblock tracer diffusion near the ODT demonstrated good agreement with experiments on quenched samples.^{6,8} More recent experimental work⁹ employed a more segregated PEP-PEE4 matrix. The corresponding tracer D/D_0 values were found to be T -independent, and $\approx 0.012 \pm 0.004$ (PEP-PEE4), 0.20 ± 0.05 (PEP-PEE2), and 0.6 ± 0.1 (PEP-PEE1). Quantitative application of our theory (with PRISM input) is technically involved and will be discussed elsewhere.²⁴ However, semiquantitative analysis is very simple. Since the T dependence of D/D_0 arises solely from the matrix concentration fluctuations, S^* , one can immediately conclude T independence is predicted for tracer diffusion in PEP-PEE4 where $T \ll T_{\text{ODT}}$. Moreover, for entangled diblock tracers shorter (N_t) than the chemically and compositionally identical matrix chains (N), the qualitative dependence of D/D_0 on tracer molecular weight follows from a power counting analysis of the known dependence on N_t of $\Delta g(\sigma)$ and $\omega(k)$ in eq 2, which yields $J \propto (N_t/N)^{7/2}$. Equivalently, the reduced tracer diffusion constant can be expressed in terms of the analogous self-diffusion ratio as $D/D_0 \approx \{1 + (N_t/N)^{7/2}[(D_0/D)_{\text{self}} - 1]\}^{-1}$. Thus, on the basis of the experimental⁹ $(D_0/D)_{\text{self}} = 90 \pm 30$ for PEP-PEE4, we predict $D/D_0 \approx 0.17 \pm 0.05$ (PEP-PEE2) and

0.5 ± 0.1 (PEP-PEE1), which are remarkably consistent with experiment. Tracer data for PEP-PEE3 are not available, but we predict $D/D_0 \approx 0.035 \pm 0.012$. Physically, the reduced diffusion constant suppression for shorter tracers is due to the smaller frictional penalty required to dynamically transport A (B) tracer segments through B (A) matrix microdomains.

The theory can be extended to treat the consequences of composition [anisotropic diffusion is of far less concern (irrelevant) for cylindrical (spherical) microphases], block friction constant asymmetry, chain stretching, dilution by neutral solvent, and matrix constraint release.²⁴ Both homopolymer and diblock tracer diffusion can also be addressed.¹¹ PMC theory can be generalized to finite frequencies, thereby allowing treatment of concentration fluctuation effects on early time (anomalous) diffusion, the unentangled-entangled crossover, and chain internal mode dynamics. Finally, we caution that the cage-averaged isotropic dynamics approach is expected to eventually fail, perhaps at very high degrees of segregation and/or for situations of strongly spatially dependent local friction.

Acknowledgment. This work was supported by grant NSF-DMR-89-20538 and the DOE-BES program in cooperation with Oak Ridge National Laboratories. We thank Professor T. P. Lodge for sending preprints, data, and stimulating discussion.

References and Notes

- (1) Bates, F. S.; Fredrickson, G. H. *Annu. Rev. Phys. Chem.* **1990**, *41*, 525.
- (2) Fredrickson, G. H.; Bates, F. S. *Annu. Rev. Mat. Sci.* **1996**, *26*, 503. Colby, R. H. *Curr. Opin. Colloid Interface Sci.* **1996**, *1*, 454.
- (3) Fredrickson, G. H.; Helfand, E. *J. Chem. Phys.* **1987**, *87*, 697. Brazovskii, S. A. *Sov. Phys. JETP* **1975**, *41*, 85. Leibler, L. *Macromolecules* **1980**, *13*, 1602.
- (4) For reviews see: Schweizer, K. S.; Curro, J. G. *Adv. Chem. Phys.* **1997**, *98*, 1. Schweizer, K. S.; Curro, J. G. *Adv. Polym. Sci.* **1994**, *116*, 319.
- (5) David, E. F.; Schweizer, K. S. *J. Chem. Phys.* **1994**, *100*, 7767, 7784.
- (6) Dalvi, M. C.; Eastman, C. E.; Lodge, T. P. *Phys. Rev. Lett.* **1993**, *71*, 2591.
- (7) Eastman, C. E.; Lodge, T. P. *Macromolecules* **1994**, *27*, 5591.
- (8) Dalvi, M. C.; Lodge, T. P. *Macromolecules* **1994**, *27*, 3487.
- (9) Lodge, T. P.; Dalvi, M. C. *Phys. Rev. Lett.* **1995**, *75*, 657.
- (10) Tang, H.; Schweizer, K. S. *J. Chem. Phys.* **1996**, *105*, 779.
- (11) Tang, H.; Schweizer, K. S. *J. Chem. Phys.* **1995**, *103*, 6296.
- (12) Schweizer, K. S. *J. Chem. Phys.* **1989**, *91*, 5802, 5822.
- (13) Schweizer, K. S.; Szamel, G. *Trans. Theory Stat. Phys.* **1995**, *24*, 946.
- (14) Fredrickson, G. H.; Milner, S. T. *Mater. Res. Soc. Symp. Proc.* **1990**, *177*, 169. Barrat, J.-L.; Fredrickson, G. H. *Macromolecules* **1991**, *24*, 6378.
- (15) Guenza, M.; Schweizer, K. S. *J. Chem. Phys.* **1997**, *106*, 7391.
- (16) Shull, K. R.; Kramer, E. J.; Bates, F. S.; Rosedale, J. H. *Macromolecules* **1991**, *24*, 1383.
- (17) David, E. F.; Schweizer, K. S. *J. Chem. Soc., Faraday Soc.* **1995**, *91*, 2411.
- (18) Leibig, C. M.; Fredrickson, G. H. *J. Poly. Sci., Polym. Phys.* **1996**, *34*, 163.
- (19) Genz, U.; Vilgis, T. A. *J. Chem. Phys.* **1994**, *101*, 7111.
- (20) Ackasu, A. Z.; Benmouna, M.; Benoit, H. *Polymer* **1986**, *27*, 1935.
- (21) de Gennes, P. G. *Scaling Concepts in Polymer Physics*; Cornell University: Ithaca, NY, 1978.
- (22) Fuchs, M.; Schweizer, K. S. *J. Chem. Phys.* **1997**, *106*, 347.
- (23) Brown, W.; Nicolai, T. *Colloid Polym. Sci.* **1990**, *268*, 977; Fetters, L. J.; Lohse, D.; Richter, D.; Witten, T.; Zirkel, A. *Macromolecules* **1994**, *22*, 4639.
- (24) Tang, H.; Guenza, M.; Schweizer, K. S. Manuscript in preparation.